Available online at www.sciencedirect.com

ScienceDirect

Proceedings of the Combustion Institute 36 (2017) 1929–1935

Proceedings of the Combustion Institute

www.elsevier.com/locate/proci

# Multiscale analysis of turbulence-flame interaction in premixed flames

N.A.K. Doan [a,*], N. Swaminathan [a], N. Chakraborty [b]

[a] *Department of Engineering, University of Cambridge, Trumpington Street, Cambridge CB2 1PZ, United Kingdom*
[b] *School of Mechanical and Systems Engineering, Newcastle University, Claremont Road, Newcastle-Upon-Tyne NE1 7RU, United Kingdom*

Received 2 December 2015; accepted 26 July 2016
Available online 28 September 2016

**Abstract**

Multiscale analysis of turbulence–flame interaction is performed using direct numerical simulation (DNS) data of premixed flames. Bandpass filtering method is used to educe turbulent eddies of various sizes and their vorticity and strain rate fields. The vortical structures at a scale of $L_\omega$ are stretched strongly by the most extensional principal strain rate of eddies of scale $4L_\omega$, which is similar to the behaviour in non-reacting turbulence. Hence, combustion does not influence the physics of vortex stretching mechanism. The fractional contribution from eddies of size $L_s$ to the total tangential strain rate is investigated. The results highlight that eddies larger than two times the laminar flame thermal thickness contributes predominantly to flame straining and eddies smaller than $2\delta_{th}$ contributes less than 10% to the total tangential strain rate for turbulence intensities, from $u'/s_L = 1.41$ to $u'/s_L = 11.25$, investigated here. The cutoff scale identified through this analysis is larger than the previous propositions and the implication of this finding to subgrid scale premixed combustion modelling is discussed.



*Keywords:* Direct numerical simulation (DNS); Turbulent premixed flame; Flame–turbulence interaction; Multiscale decomposition; Flame tangential strain rate

## 1. Introduction

Most of practical combustion occurs in turbulent flows involving a strong nonlinear coupling between turbulence and chemical processes, and the flame is wrinkled and strained by turbulent eddies [1–4]. The flame wrinkling and straining are caused respectively by vorticity and strain-dominated structures in turbulence [5,6]. The heat release from combustion changes fluid properties such as density and viscosity and they in turn affect the turbulence. Hence, the turbulence-flame interaction is a two-way coupling. The premixed combustion is a small scale phenomenon having the laminar flame thermal thickness and burning veloc-

* Corresponding author. Fax: +44 1223 339906.
*E-mail address:* nakd2@cam.ac.uk (N.A.K. Doan).

http://dx.doi.org/10.1016/j.proci.2016.07.111

ity as its representative scales while the turbulence involves a spectrum of scales ranging from energy containing, integral, to viscous, Kolmogorov, scales. One can query if the whole spectrum of these scales imparts influences on the flame physics or only a certain part of this spectrum influences the flame predominantly. This classical question has been raised in many earlier studies and it has been suggested that the Gibson scale may be an appropriate cutoff scale [1], and Kolmogorov scale are too weak to wrinkle or strain the flame [7,8]. Our interest here is from the perspective of combustion modelling for large eddy simulation (LES).

A key modelling quantity resulting from the turbulence–flame interaction is the flame stretch, $\kappa$, which is a measure for the change of elemental flame area, $\delta A$, given by [9]:

$$\kappa = \frac{1}{\delta A}\frac{d\,\delta A}{dt} = \left(\delta_{ij} - n_i n_j\right)e_{ij} + s_d\frac{\partial n_i}{\partial x_i} = a_T + s_d\,K_m \quad (1)$$

where $\delta_{ij}$ is the Kronecker delta, $n_i$ is the component in spatial direction $x_i$ of the flame normal vector $\mathbf{n} = -\nabla\mathbf{c}/|\nabla\mathbf{c}|$ with $c$ as a reaction progress variable based on fuel mass fraction, $s_d = (Dc/Dt)/|\nabla c|$ is the displacement speed as defined in [1], and $e_{ij} = 0.5\left(\partial u_i/\partial x_j + \partial u_j/\partial x_i\right)$ is the strain tensor with $u_i$ being the turbulent velocity component in the direction $i$. The tangential strain rate, $a_T$, and the curvature, $K_m$, coming from flame wrinkling are defined by Eq. (1). The flame stretch is typically taken as a source for flame surface area in the context of Flame Surface Density (FSD) formulation [10,11] and there is a possibility for the surface averaged stretch to be negative [12–14]. The stretch is used to obtain the flame wrinkling in LES for the thickened flame model [15,16] and is also required to determine the local flame propagation speed in the $G$ equation approach [17]. Various approaches such as strained flamelets and efficiency function have been proposed in the past for both Reynolds Averaged Navier-Stokes (RANS) [18,19] and LES [15,16,20] calculations of premixed combustion, and these approaches work well for RANS calculations. Since most of the dynamic scales are resolved in LES, the inclusion of the flame stretch induced by subgrid eddies may not be required in these approaches because these eddies may be too weak to stretch the flame.

These formulations mentioned above were proposed based on a general picture that large scales stretch the flame while small scales merely broaden the preheat zone. Nevertheless, this is only a conjecture which is yet to be validated. The Kolmogorov scales were noted to have lower efficiency for flame stretching [7,8] but another study [21] suggested that this scale produced the highest stretch. Taylor timescale was also suggested to be an appropriate scaling factor for the tangential strain rate [22,23]. These qualitative arguments were based on tests using flows such as counter rotating vortices or a weak homogeneous turbulence (with low intensity) interacting with a premixed flame. The hydrogen-air flames of [22,23] include thermo-diffusive instabilities which will affect the flame-turbulence interaction. The efficiency function [19] approach was developed using premixed flame interacting with two-dimensional counter rotating vortices, which was developed further for LES [15,16]. However, turbulent flows involve non-linear interaction of spectrum of scales (or eddies) having complex morphology and topology which could challenge the presumption that the stretch efficiency can be taken to be well described by an ensemble of interactions between pairs of counter-rotating vortices. Indeed, measurements of Steinberg and Driscoll [5,6] showed that the flame stretching produced by turbulent flows is not described well by this canonical flow. These contradictory views and qualitative analyses raise two questions, viz., (1) what is the smallest turbulence scale imparting significant flame stretch? and (2) what is its implication for modelling of filtered reaction rate in LES? The vortical structures are produced by vortex stretching mechanism in turbulence and hence the influence of turbulence-flame interaction on this mechanism is also of interest. The aim of this study is to find answers to these questions by analysing Direct Numerical Simulation (DNS) data of premixed flames using a multiscale analysis called bandpass filtering technique.

The DNS data used for this analysis are described in Section 2 and bandpass filtering technique is discussed in Section 3. The results are presented and discussed in Section 4, and conclusions are summarised in the final section.

## 2. DNS data

Five sets of turbulent premixed flame DNS data [24–26] are analysed here. These simulations considered a premixed flame propagating into homogeneous turbulence in the reactant mixture flowing from left to right in Fig. 1, which will be discussed in detail later. The various characteristics of these data are listed in Table 1. The turbulent Reynolds number, Re, is based on the integral length scale $\ell$ and the root mean square of turbulent velocity fluctuation $u'$ entering the computational domain. The laminar burning velocity is $s_L$ and the thermal thickness is $\delta_{th}$. The Damkohler number is $\mathrm{Da} = \ell\, s_L/(\delta_{th}u')$ and the Karlovitz number is $\mathrm{Ka} = (u'/s_L)^{3/2}(\delta_{th}/\ell)^{1/2}$. The combustion conditions of these five flames span from corrugated-flamelet to the thin reaction zones in the regime diagram of Peters [1] as shown inFig. 2. The flame of Rutland and Cant [24] is in the corrugated-flamelet regime and that of Minamoto et al. [25] is in the lower part of the thin reaction zones regime. The cases from

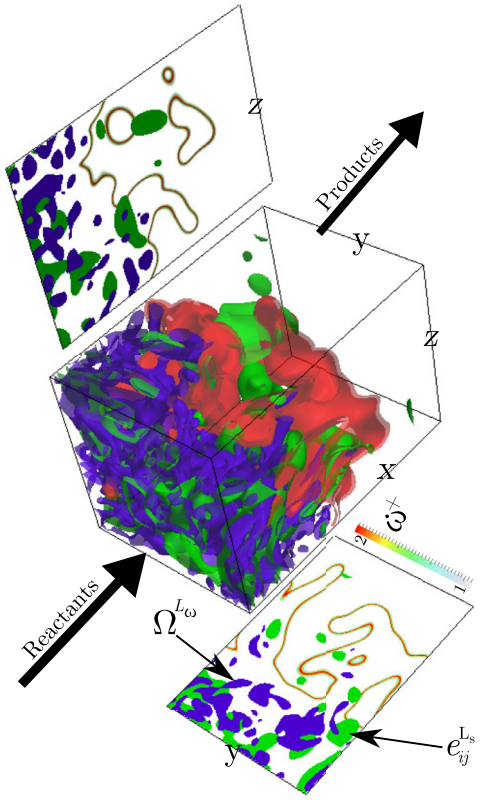


Fig. 1. Reaction rate of $c$ with bandpass filtered strain rate $e_{ij}^{L_s}$, at $L_s \approx 3.3\delta_{th}$ and enstrophy $\Omega^{L_\omega}$, at $L_\omega = \delta_{th}$, fields for $u'/s_L = 11.25$ case in Table 1, $x-z$ and $x-y$ cuts are shown.

Table 1
DNS data attributes.

| $u'/s_L$ | $\ell/\delta_{th}$ | Re | Da | Ka | Ref. |
|---|---|---|---|---|---|
| 1.41 | 6.16 | 56.7 | 4.37 | 0.67 | [24] |
| 2.19 | 2.11 | 38.5 | 0.97 | 2.22 | [25] |
| 7.5 | 2.45 | 47.0 | 0.33 | 13.2 | [26] |
| 9.0 | 4.31 | 100.0 | 0.48 | 13.0 | [26] |
| 11.25 | 3.75 | 110.0 | 0.33 | 19.5 | [26] |

Gao et al. [26], first described in Chakraborty et al. [27], are in the upper part of the thin reaction zones regime. A single-step chemistry is used for the DNS of Rutland and Cant [24] and Gao et al. [26], which is sufficient for the analysis of this data because the focus is on kinematic aspects of the turbulence-flame interaction. The skeletal mechanism of Smooke [28] was used by Minamoto et al. [25] and thus the analysis of this data will give first glimpses on the influence of chemistry on the present findings. Elaborate information on these datasets is available in the references cited above.

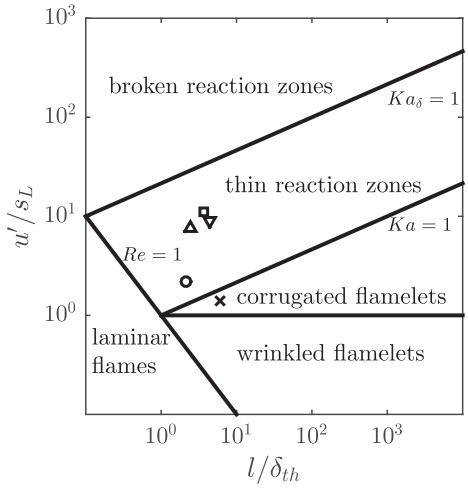


Fig. 2. Combustion regime diagram showing conditions of flames in [24] ×, [25] ∘, [26] △, ▽, □.

Also these data have been used in previous studies [29,30] to investigate velocity and scalar gradients in premixed flames and thus the numerical resolution used for those simulations is good to address the objectives of this study. It should be further noted that for the data from [26], the mesh size is such that the grid spacing is either smaller or equal to the Kolmogorov length scale which is enough to resolve the scales of turbulence under study here. Finally, the range of turbulence Reynolds numbers considered here is similar to those observed in typical laboratory-scale premixed flames or flows in IC engines or stationary gas turbine combustors (see Fig. 1.3 of [31] or Fig. 3 of [32]).

## 3. Bandpass filtering

In order to calculate the flame stretch induced by eddies of a given size $L$, one needs to educe them from the spectrum of eddies present in turbulence. The bandpass (not LES) filtering method allows one to achieve this by suppressing eddies which are smaller and larger than $L$. This procedure is described by Leung et al. [33] and the essential steps involved are summarised briefly here. First, the turbulent velocity field at a given time is Fourier transformed and then the Fourier coefficients are multiplied by a transfer function $T_b(h) = \sqrt{8/L}\, h^2 \exp(-h^2)$ with $h = kL/2$, where $k = |\mathbf{k}|$ is the magnitude of the wavenumber, to obtain the Fourier coefficients of the bandpass filtered field, $\widehat{\mathbf{u}}_b^L$. Then, inverse Fourier transform is used to obtain the bandpass filtered velocity field, $\mathbf{u}_\mathbf{b}^\mathbf{L}$, in physical space. The eddies which are much larger and smaller than $L$ are suppressed by this method and the field $\mathbf{u}_\mathbf{b}^\mathbf{L}$ have eddies of size around $L$ pre-

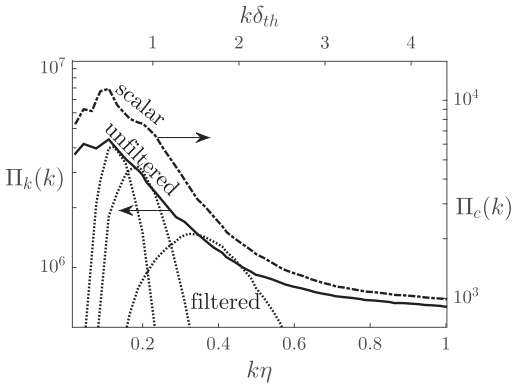


Fig. 3. Compensated energy spectrum for unfiltered and filtered at $L = 15\eta$, $10\eta$ and $5\eta$ (left to right) velocity fields and unfiltered progress variable.

dominantly. Interested readers are referred to Ref. [33] for detailed information on this procedure. The strain rate, $e_{ij}^L$, and vorticity $\boldsymbol{\omega}^L = \nabla \times \mathbf{u_b^L}$ at scale $L$ are obtained using $\mathbf{u_b^L}$ and this strain rate is used in Eq. (1) to get the tangential strain rate induced by the eddies of size $L$. These steps are repeated for $0.1\delta_{th} \leq L \leq 20\delta_{th}$ to get the tangential strain rate, $a_T^L$, contribution from eddies of scale $L$.

## 4. Results and discussions

The compensated turbulent kinetic energy spectrum $\Pi_k(k) = E(k)k^{5/3}\epsilon^{-2/3}$, where $\epsilon$ is the turbulent kinetic energy dissipation rate, is presented in Fig. 3 for the unfiltered and three bandpass filtered velocity fields for the highest $u'/s_L$ case in Table 1. The filtered fields have $L = 15\eta$, $10\eta$ and $5\eta$ and the peak energy is at $\sqrt{5}/L$ [33]. As expected, the energy in the filtered field is centred around the chosen length scale and the energies of larger and smaller eddies are attenuated. The spectrum of the unfiltered field is the envelop of the peaks in the filtered spectra. The compensated energy spectrum, $\Pi_c$, of the scalar, $c$, is also shown in Fig. 3, which has the peak at $k\delta_{th} \approx 0.49(k\eta = k\delta_{th}\mathrm{Ka}^{-1/2} \approx 0.11)$. These results are similar for the other flames in Table 1. It should be noted that only a small inertial range is observed on the unfiltered spectrum as a result of the limited range of scales and Reynolds numbers of the present data. However, this does not affect the conclusion of this study as the flame scale is very much smaller than the scales of the inertial range. Furthermore, what really matters for the multiscale analysis is the presence of some scales and their relative range.

Typical spatial distribution of the filtered structures are shown in Fig. 1 with contours of normalised progress variable reaction rate, $\dot{\omega}^+$ which is threshold at $\dot{\omega}^+ = 1$ for its iso-surface shown in Fig. 1. The reaction rate is normalised using $\rho_u s_L/\delta_{th}$, where $\rho_u$ is the reactant density. The strain rate, $e_{ij}^{L_s}$, structures have a scale $L_s = 14.6\eta \approx 3.3\delta_{th}$ and the vortical structures identified using enstrophy, $\Omega^{L_\omega} = 0.5|\boldsymbol{\omega}^{L_\omega}|^2$ where $\boldsymbol{\omega}^{L_\omega}$ is the vorticity vector, having $L_\omega = 4.4\eta \approx \delta_{th}$. Turbulent structures presented in Fig. 1 are threshold at their respective mean plus half standard deviation value. It can be observed in the plane cuts in Fig. 1 that downstream of the flame, less and sparser structures of $\Omega^{L_\omega}$ and $e_{ij}^{L_s}$ are found suggesting that the flame dampens the turbulence. Furthermore, variations in the distribution and sizes of these structures are observed suggesting that their effects on the flame will be different [3,21,34]. Indeed, strain rate structures can be found in both upstream and downstream of the flame front, even in its neighbourhood, whereas the enstrophy structure representing small scales are present predominantly in far upstream of the flame. This implies that small scale structures may have a reduced influence on the flame. This will be discussed in further detail later in Section 4.2. Furthermore, it is important to analyse the effect of the flame on the vortex stretching mechanism which produces these small scales.

### 4.1. Influence of combustion on vortex stretching

It is well accepted that vortex stretching produces eddies of various scales and the classical picture suggests that eddies of smaller size are produced by the stretching and subsequent breaking of larger eddies. This physical mechanism can be elucidated by studying the alignment between the vorticity vector, $\boldsymbol{\omega}$, and principal components of strain rate tensor. The most extensional, the most compressive and intermediate principal components are denoted by $\alpha$, $\gamma$ and $\beta$ respectively. Thus, the enstrophy production is $\omega_i e_{ij} \omega_j = \omega_i \omega_i \left(\alpha \cos^2\theta_\alpha + \beta \cos^2\theta_\beta + \gamma \cos^2\theta_\gamma\right)$, where $\theta_i$ is the angle between $\boldsymbol{\omega}$ and the direction of the principal strain rate $i$ [33]. The vorticity has to align with $\alpha$ or positive part of $\beta$ to produce enstrophy through stretching and indeed the alignment with $\beta$ was observed if the eddies were unfiltered [35]. Similar behaviour was observed for premixed flames also [36]. The bandpass filtering analysis by Leung et al. [33] showed that the vorticity with scale $L_\omega$ aligned with $\alpha$ of scales $L_s > L_\omega$ and the enstrophy production was maximum when $L_s \simeq 4L_\omega$.

The pdf (probability density function) of $|\cos\theta_i|$ for $\alpha$ and $\beta$ strain rates for the bandpass filtered fields of premixed flame with $u'/s_L = 11.25$ is shown in Fig. 4 for $L_\omega = \delta_{th}$ and $0.5\delta_{th} \leq L_s \leq 10\delta_{th}$. These pdfs are extracted from the entire computational domain. Similar to the non-reacting flow results in [33], a preferential alignment of $\boldsymbol{\omega}$ is found with $\alpha$ from eddies larger than the vortical structure and the alignment with $\beta$ is approached when $L_s \leq L_\omega$. The probability, $P$, for $0.98 \leq |\cos\theta_\alpha| \leq 1$

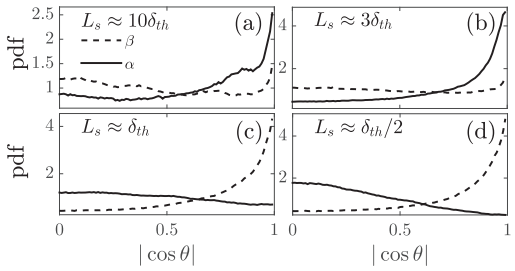


Fig. 4. PDF of the magnitudes of direction cosines between vorticity at $L_\omega = \delta_{th}$ and principal strain rates at $L_s$ in the case with $u'/s_L = 11.25$.

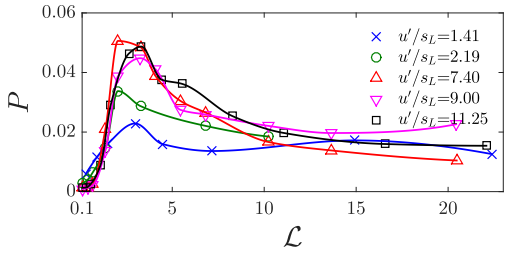


Fig. 5. Probability of perfect alignment between the vorticity at $L_\omega$ and $\alpha$ strain rate at $L_s = \mathcal{L}L_\omega$.

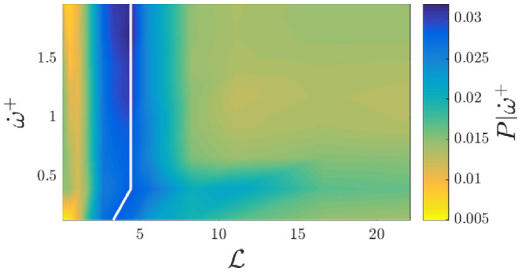


Fig. 6. Probability of perfect alignment between the vorticity at $L_\omega$ and $\alpha$ strain rate at $L_s = \mathcal{L}L_\omega$ conditioned on $\dot{\omega}^+$ with the maximum probability shown (white line) for case with initial $u'/s_L = 11.25$.

as a function of $\mathcal{L} = L_s/L_\omega$ is shown in Fig. 5 for all the flames in Table 1 to quantify an eddy scale imparting the most stretching on vortical structures of scale $L_\omega$. The peak occurs for $\mathcal{L}$ between 3 and 4 for the flames, implying that the vortical structure is stretched mostly by structures 3 to 4 times bigger than itself, which was also observed in [33].

In order to assess the role of reaction on this alignment statistics more effectively, the alignment pdfs conditioned on the reaction rate can be investigated. This is done through the joint-pdf of $\psi = |\cos\theta_\alpha|$ and $\dot{\omega}^+$, noted as $p_{\psi,\dot{\omega}^+}$, and computing $P$ conditioned on $\dot{\omega}^+$ for the various $\mathcal{L}$ using $P|\dot{\omega}^+ = \int_{0.98}^{1} p_{\psi,\dot{\omega}^+} d\psi / p_{\dot{\omega}^+}$ with $p_{\dot{\omega}^+}$ as the marginal pdf. Figure 6 shows this result. It can be observed that the reaction rate does not have a strong influence on the behaviour previously mentioned as the maximum probability $P$ is found for $3 \leq \mathcal{L} \leq 5$ for all reaction rates.

The similarity between the present reacting and non-reacting [33] results suggests that the mechanism of vortex stretching and the role of relative eddy sizes on this mechanism are not unduly influenced by the presence of chemical reactions and heat release. Hence, the vortex stretching mechanism is expected to play a key role in turbulent flows. Other mechanisms such as baroclinic torque for enstrophy production [3,21,34] are not considered because the main focus is on the eddy-interaction and vortex stretching mechanism in reacting turbulence.

### 4.2. Multiscale analysis of tangential strain rate

As noted in Section 3, the bandpass filtering technique is used to calculate the tangential strain imparted by eddies of scale $L_s$ through $a_T^{L_s} = (\delta_{ij} - n_i n_j) e_{ij}^{L_s}$ and its surface averaged value is

$$\psi(L_s^+) = \langle |\nabla c| a_T^{L_s^+} \rangle / \langle |\nabla c| \rangle, \tag{2}$$

where $L_s^+ = L_s/\delta_{th}$ and $\psi_{\text{int}} = \int_0^\infty \psi \, dL_s^+$ gives the surface averaged contribution coming from all eddies in the flow. Figure 7a shows the variation of fractional contribution, $\widehat{\psi} = \psi/\psi_{\text{int}}$, with $L_s^+$. The peak contribution is for $5 \leq L_s^+ \leq 8$ in the corrugated flame with $u'/s_L = 1.41$. The flame with $u'/s_L = 2.19$ and a skeletal mechanism also has peak $\widehat{\psi}$ from similar sized eddies of $6 \leq L_s^+ \leq 10$ suggesting that the chemical mechanism does not play a significant role in the kinematic aspect of flame-turbulence interaction. There are no data for eddies larger than $13\delta_{th}$ for the flame with $u'/s_L = 2.19$ because larger structures are bigger than the computational domain, however, the decreasing trend is seen already. Furthermore, the length scale ratio, $\ell/\delta_{th}$, does not seem to influence this behaviour unduly when $u'/s_L$ is similar. The peak value is shifted towards $L_s^+$ of about 2 to 3 for flames with higher turbulence intensity. Furthermore there is a sharp decrease in contributions from eddies of smaller size whereas the decrease is slower for larger scales up to $L_s^+ \simeq 17$. This suggests that eddies in the range $3 \leq L_s^+ \leq 17$ have substantial effect on flame straining. This is confirmed further by the cumulative integral $\psi^* = \int_0^{L_s^+} \widehat{\psi} dL_s^+$ plotted in Fig. 7b. There is less than 20% contribution from eddies smaller than $3\delta_{th}$ and less than 10% for eddies larger than $17\delta_{th}$.

Roberts et al. [8] defined a cutoff scale, $l_R$, given by

$$(l_R/\delta_{th}) = 2.0\left(u'/s_L\right)^{-3/4} (\ell/\delta_{th})^{1/4}, \tag{3}$$

and eddies smaller than $l_R$ are thought to have nearly no impact on flame wrinkling and straining. Also, Gibson scale $l_G = s_L^3/\epsilon$, where $\epsilon$ is the

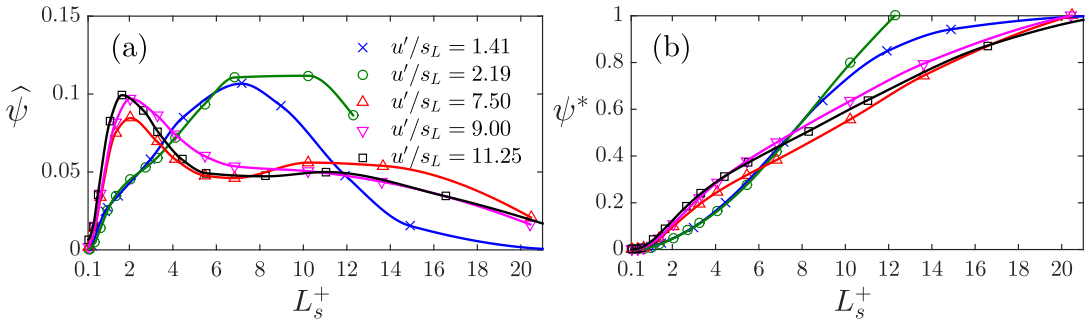


Fig. 7. (a) Surface averaged tangential strain rate from eddies of scale $L_s^+$ normalised by total contribution and (b) its cumulative integral.

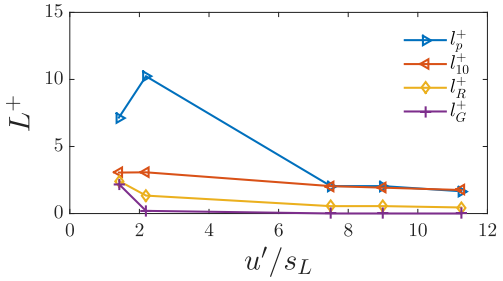


Fig. 8. Comparison of various cutoff scales.

turbulent kinetic energy dissipation rate, was suggested to be the smallest eddy size that can interact effectively with flame [37]. These cutoff scales, normalised by $\delta_{th}$, are compared in Fig. 8 for the five flames along with length scales corresponding to $\psi^* = 0.1$ and peak $\widehat{\psi}$. These two scales are $l_{10}^+$ and $l_p^+$ respectively, and $l_{10}^+$ implies that eddies smaller than $l_{10}^+$ contribute 10% or smaller to the total tangential strain rate experienced by the flame. The $l_p^+$ is about 10 for $u'/s_L = 2.19$ and it approaches $l_{10}^+$ as $u'/s_L$ increases. The results in Fig. 8 suggest that the range of eddies having weak influence in straining the flame is larger than that originally thought.

This result has wider implications for LES combustion modelling. Indeed, this analysis has shown that eddies of sizes larger than $2\delta_{th}$ imparted the most influence on the flame and it may not be required to resolve scales smaller than this in LES. The bandpass filter used is efficient in cutting scales smaller than the specified one and cuts larger scales less sharply. As a consequence the values found here for $l_p^+$ and $l_{10}^+$ are conservative because $a_T^{L_s^+}$ includes contributions from eddies of sizes $L_s^+$ and slightly larger. This suggests that LES numerical grid resolving turbulence down to $l_p^+$ or $l_{10}^+$ would capture the flame stretching quite well and it may not be necessary to use a refined model for this aspect. This is of practical importance because LES meshes typically resolve reacting turbulence down to a size of the order of $\delta_{th}$ [17]. This finding is consistent with the inner cut-off scale estimates based on fractal analysis found in several previous studies in the context of FSD [38,39] and scalar dissipation rate [26] closures.

## 5. Conclusions

Multiscale analysis of turbulent premixed flames using five DNS data is performed employing bandpass filtering technique, which allows to educe eddies of a given scale present in the turbulence spectrum. This allows us to investigate the influence of eddies of size $L_s$ on turbulence-flame interaction. The statistics of vorticity-strain alignment of eddies at various scales are studied. It is observed that vortical structures of scale $L_\omega$ are stretched by larger eddies with the maximum stretching from eddies of scale about $4L_\omega$. This is similar to non-reacting turbulence [33], which suggests that the premixed flame has negligible influence on the vortex stretching mechanism.

The influence of eddy on turbulence-flame interaction is investigated using surface averaged tangential strain rate imparted by the eddy. It is shown that eddies smaller than $2\delta_{th}$ contribute less than 10% of the total tangential strain rate and eddies larger than $17\delta_{th}$ contributes less than 10%. This has implication for the subgrid modelling for LES of premixed combustion. Indeed, these results suggest that resolving turbulence scales down to few multiples of $\delta_{th}$ would be enough to capture most of the flame straining caused by turbulence. These will be captured by the LES equations and additional modelling may not be required for subgrid scale flame stretching.

Here, only five flames covering a limited range of turbulence intensity and Re are analysed and further work is needed to assess this finding for larger turbulence intensity. As noted in Section 4, only a limited inertial range is observed in the current data and future work may be devoted to as-

sessing whether the current result can be extended to combustion at higher Re and in flows with shear and swirl, which are common in practical combustors.

## Acknowledgements

N.A.K.D. acknowledges the financial support of the Qualcomm European Research Studentship Fund in Technology. N. C. acknowledges the financial support of EPSRC.

## References

[1] N. Peters, *Turbulent Combustion*, Cambridge University Press, Cambridge, 2000.
[2] K.N.C. Bray, R.S. Cant, *Proc. R. Soc. London A* 434 (1890) (1991) 217–240.
[3] P.E. Hamlington, A.Y. Poludnenko, E.S. Oran, *Phys. Fluids* 23 (12) (2011) 125111, doi:10.1063/1.3671736.
[4] T. Poinsot, D. Veynante, *Theoretical and Numerical Combustion*, third ed., Aquaprint, 2011.
[5] A.M. Steinberg, J.F. Driscoll, *Combust. Flame* 156 (12) (2009) 2285–2306, doi:10.1016/j.combustflame.2009.06.024.
[6] A.M. Steinberg, J.F. Driscoll, *Combust. Flame* 157 (7) (2010) 1422–1435, doi:10.1016/j.combustflame.2010.02.024.
[7] T. Poinsot, D. Veynante, S. Candel, *J. Fluid Mech.* 228 (1991) 561–606, doi:10.1017/S0022112091002823.
[8] W. Roberts, J. Driscoll, M. Drake, L. Goss, *Combust. Flame* 94 (1–2) (1993) 58–69, doi:10.1016/0010-2180(93)90019-Y.
[9] S.M. Candel, T. Poinsot, *Combust. Sci. Technol.* 70 (1–3) (1990) 1–15, doi:10.1080/00102209008951608.
[10] D. Veynante, L. Vervisch, *Prog. Energy Combust. Sci.* 28 (2002) 193–266, doi:10.1016/S0360-1285(01)00017-X.
[11] E. Hawkes, R. Cant, *Combust. Flame* 126 (01) (2001) 1617–1629, doi:10.1016/S0010-2180(01)00273-5.
[12] N. Chakraborty, M. Klein, R.S. Cant, *Proc. Combust. Inst.* 31 (1) (2007) 1385–1392, doi:10.1016/j.proci.2006.07.184.
[13] S. Ruan, N. Swaminathan, Y. Mizobuchi, *Combust. Sci. Technol.* 186 (3) (2014) 243–272, doi:10.1080/00102202.2013.877335.
[14] C. Dopazo, L. Cifuentes, J. Martin, C. Jimenez, *Combust. Flame* 162 (5) (2015) 1729–1736, doi:10.1016/j.combustflame.2014.11.034.
[15] O. Colin, F. Ducros, D. Veynante, T. Poinsot, *Phys. Fluids* 12 (2000) (2000) 1843–1863, doi:10.1063/1.870436.
[16] F. Charlette, C. Meneveau, D. Veynante, *Combust. Flame* 131 (02) (2002) 159–180, doi:10.1016/S0010-2180(02)00401-7.
[17] H. Pitsch, *Annu. Rev. Fluid Mech.* 38 (1) (2006) 453–482, doi:10.1146/annurev.fluid.38.050304.092133.
[18] H. Kolla, N. Swaminathan, *Combust. Flame* 157 (5) (2010) 943–954, doi:10.1016/j.combustflame.2010.01.018.
[19] C. Meneveau, T.J. Poinsot, *Combust. Flame* 86 (4) (1991) 311–332, doi:10.1016/0010-2180(91)90126-V.
[20] E. Knudsen, H. Kolla, E.R. Hawkes, H. Pitsch, *Combust. Flame* 160 (12) (2013) 2911–2927, doi:10.1016/j.combustflame.2013.06.033.
[21] A.N. Lipatnikov, S. Nishiki, T. Hasegawa, *Phys. Fluids* 26 (10) (2014) 105104, doi:10.1063/1.4898640.
[22] Y. Nada, M. Tanahashi, T. Miyauchi, *J. Turbul.* 5 (August) (2004) 37–41, doi:10.1088/1468-5248/5/1/016.
[23] B. Yenerdag, N. Fukushima, M. Shimura, M. Tanahashi, T. Miyauchi, *Proc. Combust. Inst.* 35 (2) (2015) 1277–1285, doi:10.1016/j.proci.2014.05.153.
[24] C. J. Rutland, R. S. Cant, in: Proc. Summer Program. Cent. Turbul. Res. 1994
[25] Y. Minamoto, N. Swaminathan, R.S. Cant, T. Leung, *Combust. Flame* 161 (11) (2014) 2801–2814, doi:10.1016/j.combustflame.2014.04.018.
[26] Y. Gao, N. Chakraborty, N. Swaminathan, *Combust. Sci. Technol.* 186 (10–11) (2014) 1309–1337, doi:10.1080/00102202.2014.934581.
[27] N. Chakraborty, G. Hartung, M. Katragadda, C. Kaminski, *Combust. Flame* 158 (7) (2011) 1372–1390, doi:10.1016/j.combustflame.2010.11.014.
[28] M.D. Smooke, V. Giovangigli, M.D. Smooke, Reduc. Kinet. Mech. Asymptot. Approx. Methane-Air Flames, Lecture Notes in Physics, 384, Springer, Berlin/Heidelberg, 1991, pp. 1–28, doi:10.1007/BFb0035362.
[29] N. Swaminathan, R.W. Grout, *Phys. Fluids* 18 (4) (2006) 045102, doi:10.1063/1.2186590.
[30] Y. Minamoto, N. Swaminathan, *Combust. Flame* 161 (4) (2014) 1063–1075, doi:10.1016/j.combustflame.2013.10.005.
[31] N. Swaminathan, K.N.C. Bray, *Turbulent Premixed Flames*, Cambridge University Press, 2011, doi:10.1146/annurev.fluid.19.1.237.
[32] T. Poinsot, S. Candel, A. Trouvé, *Prog. Energy Combust. Sci.* 21 (95) (1996) 531–576, doi:10.1016/0360-1285(95)00011-9.
[33] T. Leung, N. Swaminathan, P.A. Davidson, *J. Fluid Mech.* 710 (2012) 453–481, doi:10.1017/jfm.2012.373.
[34] T.C. Treurniet, F.T.M. Nieuwstadt, B.J. Boersma, *J. Fluid Mech.* 565 (2006) 25–62, doi:10.1017/S0022112006002072.
[35] W.T. Ashurst, A.R. Kerstein, R.M. Kerr, C.H. Gibson, *Phys. Fluids* 30 (1987) 2343–2353.
[36] N. Chakraborty, *Eur. J. Mech. - B/Fluids* 46 (2014) 201–220, doi:10.1016/j.euromechflu.2014.01.002.
[37] N. Peters, *Proc. Combust. Inst.* 32 (1) (2009) 1–25, doi:10.1016/j.proci.2008.07.044.
[38] R. Knikker, D. Veynante, C. Meneveau, *Phys. Fluids* 16 (11) (2004) L91, doi:10.1063/1.1780549.
[39] N. Chakraborty, M. Klein, *Phys. Fluids* 20 (8) (2008) 085108, doi:10.1063/1.2969474.